ELSEVIER

Contents lists available at ScienceDirect

Coastal Engineering

journal homepage: www.elsevier.com/locate/coastaleng



Morphodynamic modeling of Fourleague Bay in Mississippi River Delta: Sediment fluxes across river-estuary-wetland boundaries

Nan Wang ^a, Qin Chen ^{b,c,*}, Kelin Hu ^d, Kehui Xu ^{e,f}, Samuel J. Bentley ^{f,g}, Jiaze Wang ^h

- ^a Department of Civil and Environmental Engineering, Northeastern University, 400 SN, Boston, MA 02115, USA
- ^b Department of Civil and Environmental Engineering, Northeastern University, 471 SN, Boston, MA 02115, USA
- ^c Department of Marine and Environmental Sciences, Northeastern University, 471 SN, Boston, MA 02115, USA
- ^d Department of River-Coastal Science and Engineering, Tulane University, New Orleans, LA, 70118, USA
- ^e Department of Oceanography and Coastal Sciences, Louisiana State University, Baton Rouge, LA, 70803, USA
- f Coastal Studies Institute, Louisiana State University, Baton Rouge, LA, 70803, USA
- g Department of Geology and Geophysics, Louisiana State University, Baton Rouge, LA, 70803, USA
- ^h School of Earth and Climate Sciences, University of Maine, Orono, ME, 04469, USA

ARTICLE INFO

Keywords: Delft3D Sediment transport Wind waves Vegetation Wetland morphology

ABSTRACT

To mitigate land losses in the Mississippi River Delta, sediment diversions are being employed to enable the flow of river water and sediments into wetlands experiencing degradation. A two-dimensional coupled flow-wave Delft3D model was used in this study to explore the hydrodynamics and sediment transport in Fourleague Bay (FLB), Louisiana, USA, which has been considered an analog site for studying the efficiency of sediment diversion projects. In-situ measurements of sediment accretion and hydrodynamic characteristics from 2015 to 2016 were utilized to calibrate and validate the morphodynamic model. The validated model was then applied to quantify sediment transport in FLB and surrounding marshes between May 2015 and May 2016. The results show that more sediment could be deposited to the surrounding marshes with high river discharges and strong winds. Thus, by strategically aligning the timing of pulses of river water from the diversion with the seasonal intensification of atmospheric forcing, it is possible to sustain and promote the growth of the surrounding wetlands. Moreover, we found that multiple sediment transport processes occurred during the entire study period, including the deposition of riverine sediment into the bay floor, direct deposition of riverine sediment in the surrounding marshes, resuspension of bay floor sediment, and redistribution of resuspended sediment to adjacent marshes and the Gulf of Mexico (GoM). The results indicate that the riverine sediment tended to be directly deposited in the marshes when the river discharge was high. During calm weather conditions and normal river discharge, FLB acted as a reservoir, storing sediment from the upper river, and later acted as a sediment source to the nearby wetlands and the GoM during energetic atmospheric conditions. This suggests that using the bay floor as a reservoir can extend the distance over which wetlands can benefit from the sediment diversions, as the supply of sediment to the wetlands becomes a multi-step process. Thus, it is important to retain sediments from river diversions in shallow bays and allow storms to redistribute them to adjacent wetlands.

1. Introduction

As one of the socio-ecologically richest systems in the world, the Mississippi River Delta (MRD) mitigates the impact of ocean waves and storm surges during extreme events, providing nesting habitats for fisheries and wildlife (Liu et al., 2018). It also enables vital marine transport to the interior of North America and supports substantial energy production for the USA. However, the MRD has been at risk of

drowning and extensive erosion, experiencing a wetland loss rate of 58 km²/yr from 1932 to 2016 (Couvillion et al., 2017), which adversely affects coastal communities and valuable economic resources. Several factors contribute to the degradation of the MRD's wetlands, including sea level rise, land subsidence, and human-induced disruption of sediment supply (Wang et al., 2018). Consequently, the state of Louisiana has implemented the Coastal Master Plan to restore, construct, and maintain coastal wetlands in the MRD (Restreppo et al., 2019). The

^{*} Corresponding author. Department of Civil and Environmental Engineering, Northeastern University, 471 SN, Boston, MA 02115, USA. *E-mail addresses*: wang.nan@northeastern.edu (N. Wang), q.chen@northeastern.edu (Q. Chen).

program includes multiple protection and restoration projects, such as the restoration of oyster reefs, barrier islands, marshes, and the implementation of sediment diversions (CPRA, 2012; CPRA, 2017; CPRA, 2023).

River-sediment diversion plays a crucial role in the Coastal Master Plan for addressing land loss in the MRD (Xu et al., 2019). The project involves the construction of structures and channels to facilitate the flow of river water and sediments from the Mississippi and Atchafalaya Rivers into degrading wetlands (CPRA, 2017; CPRA, 2023). In recent years, significant efforts have been devoted to understanding the sediment transport processes and wetland sustainability in the MRD (e.g., Meselhe et al., 2012; Rosen and Xu, 2014; Yuill et al., 2016; Elsey-Quirk et al., 2019; Bomer et al., 2019; Meselhe et al., 2021). For example, Wang et al. (2018) collected hourly data on waves, currents, and suspended sediment concentration (SSC) at a station in Fourleague Bay (FLB) in 2015 and 2016. They found that sediment resuspension in the shallow bay was primarily influenced by wind-driven waves, and the contribution of resuspended and riverine sediment to nearby wetlands was strongly correlated with seasonal changes in wind directions and river discharges. Restreppo et al. (2019) collected push cores along the bay and marsh within FLB in 2015 and 2016 and calculated inventories of ⁷Be to examine the sediment deposition rate. The findings showed that when the river discharge was high, sediment bypassed the bay floor and entered the neighboring marshes directly, which could be enhanced by cold fronts. Conversely, when the river discharge was low and atmospheric conditions were calm, riverine sediment settled directly on the bay's bottom.

Although existing studies have successfully explored the sediment contribution from river and bay beds to wetlands, more spatial explicit modeling studies are needed to gain a quantitative understanding of sediment transport and preservation in coupled estuary-wetland systems. Such studies would inform the development of more effective and nature-based strategies for coastal estuary-wetland sustainability. Previous field studies have estimated sediment transport and deposition in the bay floor and adjacent wetlands using in-situ seasonal mooring

measurements and/or transect sediment coring. However, these studies had limited spatial and temporal coverage. Therefore, extrapolating those field findings to the entire bay-wetland system on an annual scale can be challenging due to the heterogeneity of bathymetry, vegetation characteristics, and frequent pulse variations in meteorological dynamics. In contrast to field observations, numerical models can provide a powerful tool for quantitatively understanding system-wide coastal dynamic processes over long temporal scales. In this study, we applied numerical models to simulate hydrodynamics and identify sediment transport pathways in the FLB and adjacent wetlands over time to better understand the influence of sediment diversion within a coupled estuary-wetland system at a large spatiotemporal scale. It's worth noting that the shorelines near Atchafalaya Bay and Fourleague Bay have remained relatively stable over the past several decades. This contrasts with the evident coastal erosion in areas of the eastern LA coast, such as Terrebonne and Barataria bays.

Significant advancements have been achieved in the development of physics-based numerical models that rely on wave action and momentum balance principles. Among these models, the Delft3D modeling suite has gained widespread recognition as a valuable tool for accurately assessing hydrodynamics, sediment transport, and morphological changes in coastal regions (Table 1). For example, Hu et al. (2018) utilized the Delft3D model to investigate the impact of Hurricane Sandy (2012) on the morphology of salt marshes in Jamaica Bay, New York. Their findings show that the sediment introduced into the bay during the storm constituted only 1% of the overall quantity of sediment undergoing reworking within the bay. Liu et al. (2018) used Delft3D to examine the impact of sediment transport caused by Hurricane Gustav (2008) in the Barataria and Terrebonne basins, Louisiana. Their findings indicated that mud originated from the bays accounted for 98.2% of wetland deposition in Barataria Bay and 88.7% in Terrebonne Bay from the hurricane. Overall, Delft3D presents a remarkable ability to identify sediment transport pathways in the bay and wetland areas during extreme weather events. However, no studies have yet employed Delft3D to examine the impact of river-sediment diversion on

Table 1Summary of selected previous studies on simulating hydrodynamics and sediment transport using Delft3D.

Author	Study location	Time scale	Purpose	Sediment
Wenneker et al. (2011)	Duck, North Carolina	22–27 September 1994	Predict nearshore morphology change on a short-term scale	sand
Dissanayake et al. (2012)	Ley Bay area in the East Frisian Wadden Sea	1975–1990	Morphodynamic response to the construction of a peninsula	sand/mud
Boudet et al. (2017)	The mouth-lobe of the Grand Rhone	275 storm and flood events from 1979 to 2010	Analyze the sediment transport at the Rhone mouth in idealized cases	sand
Luijendijk et al. (2017)	Sand Engine	August 2011–August 2012	Examine the initial morphological response of the Sand Engine	sand
Bergillos et al. (2017)	Playa Granada	A 36-day time series of 864 sea states	Study the storm response of a mixed sand-gravel beach under varying wave directions	sand/ gravel
Yao et al. (2018)	Jiangsu coast	August–September 2006, and 2006–2007	Simulate sediment transport in a sand-silt mixed environment in both short-term and long-term scales	sand/silt
Luan et al. (2018)	Yangtze River delta	1997–2013	Study morphodynamic impacts of large-scale navigational channel engineering project in the Yangtze River delta	mud
Tonnon et al. (2018)	Sand Motor	August 2011 and September 2014	Simulate erosion rates, life span, and maintenance volumes of mega nourishments	sand
Herrling and Winter (2018)	Barrier island system in the southern North Sea	May 2004–June 2006	Simulate sediment dynamics of graded sand fractions to representative hydrodynamic conditions.	sand
van Ormondt et al. (2020)	Fire Island, New York	November 1, 2012–November 1, 2015	Hindcast the morphodynamic evolution of a barrier island breach	sand
Johnson et al. (2021)	Caminada Headlands, Louisiana	Hurricane Gustav's (2008)	Investigate the effects of land cover and limited sediment supply on low-lying barrier island morphology under storm conditions	sand
King et al. (2021)	The North Coast of Cornwall	June 2015–May 2018	Investigate environmental and morphological controls on headland sand bypassing	sand
Zhu et al. (2021)	South Bay within the Virginia Coast Reserve	January and June 2011.	Quantify seasonal seagrass impacts on bay dynamics	sand/mud
Ton et al. (2023) López-Ramade et al. (2023)	Lake Markermeer The northern coast of Yucatan, Mexico	July 2018–April 2021 May–June2017	Quantify alongshore sediment transport in a low-energy, no-tidal lake Simulate beach change near groins and submerged breakwaters	sand sand
Stevens et al. (2023)	The mouth of the Columbia River	August 28 - October 1, 2019.	Simulate dispersal of a submerged nearshore berm	sand

hydrodynamics and sediment transport within an estuary-wetland system. Thus, in this work, we applied Delft3D to achieve a better understanding of the fine sediment dispersal process using FLB as an analog site.

In this study, we utilized Delft3D to evaluate coastal wetland elevation changes by considering bay and adjacent wetlands as an entire system with high resolution. Moreover, we quantified the dynamic interaction of sediment transport between the bay and wetland over an annual scale, encompassing both storm events and fair weather conditions, while also considering the effect of vegetation on sediment deposition. Specifically, we developed a coupled flow-wave Delft3D model to explore hydrodynamics and sediment transport in FLB and adjacent wetlands between May 2015 and May 2016 with the following objectives: (1) identify the primary hydrodynamic forces that drive sediment transport, such as the Atchafalava River and/or wind-driven waves, (2) analyze and quantify the sediment contribution from different sources to adjacent wetlands, and (3) estimate the sediment flux and budget in the FLB. The rest of the paper is organized as follows. Section 2 presents the study area, measurement data, and Delft3D model setup. The model was validated by comparing the simulated and observed hydrodynamics and morphological changes in Section 3. Additionally, the spatial patterns of erosion and deposition in the FLB during the study period were analyzed in the same section. Section 4 discusses the sediment budget and the dominant hydrodynamic forces driving sediment transport in FLB. Finally, Section 5 provides a summary of our findings.

2. Methods

2.1. Study area and observations

The study site is the wetland-bay system of FLB in the MRD (Fig. 1). FLB is characterized as a shallow and vertically well-mixed estuary, covering an approximate area of 95 km² (Denes and Caffrey, 1988). The bay can be divided into two main sections. The upper and northern portion extends in a northwest to southeast direction, connecting to Atchafalaya Bay via a 2.5 km wide opening. The lower section runs in a north-south orientation and communicates with the northern Gulf of Mexico (GoM) through a tidal inlet called Oyster Bayou (Wang et al., 1995). Oyster Bayou serves as the sole direct outlet to the GoM, with peak current speeds surpassing 2 m/s (Perez et al., 2000). The surrounding area of the bay is vegetated by low-lying marshes throughout the year (Restreppo et al., 2019). Additionally, FLB is connected to the neighboring bay, Lost Lake, on the east via Blue Hammock Bayou. Given the significant size of Lost Lake, the impact of this connection on water levels, currents, and sediment budgets at FLB was also considered in this study.

FLB is strongly influenced by several factors, such as wind (e.g., cold fronts and tropical cyclones), river discharge from the Atchafalaya River, and tides from the GoM. The dominant tidal pattern in FLB is primarily diurnal with a semidiurnal component, resulting in a tidal range ranging from 0.30 to 0.48 m (Wang et al., 2018). Because of the relatively low tidal range in FLB, the impact of water level changes

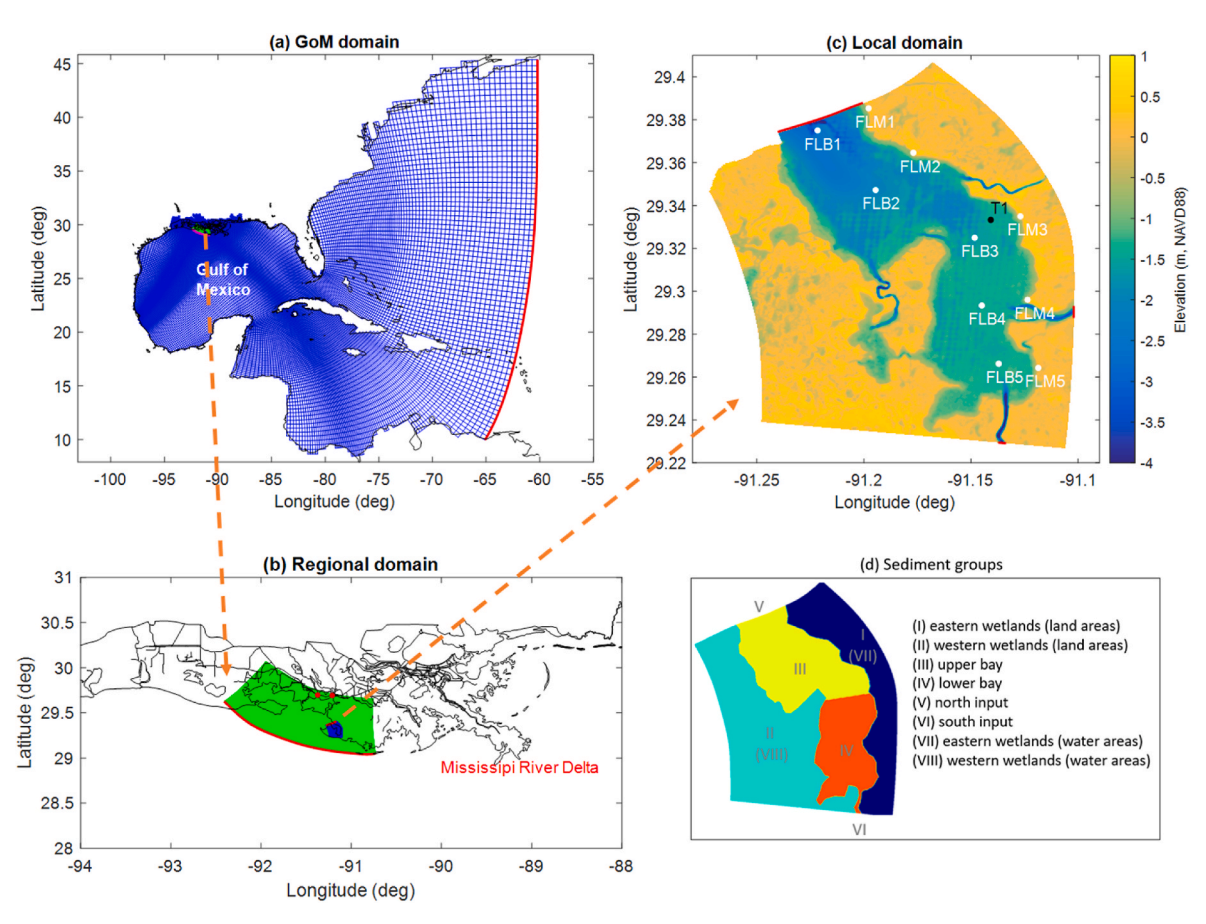


Fig. 1. Three-level computational domains and sediment groups: (a) GoM domain, (b) regional domain (black dots represent the locations of NOAA stations), and (c) local domain, including tripod station T1 and push cores locations at FLB (Fourleague Bay) and FLM (Fouleague Bay Marsh). The red lines represent the locations of boundaries in different computational domains. (d) Sediment groups in the local domain simulation.

caused by wind forces during storm events can be more significant than that of tides (Perez et al., 2000). Although the estuary receives less than 5% of the total discharge from the Atchafalaya River (Lane et al., 2011), the surrounding wetlands remain relatively stable without significant erosion or progradation during past several decades (Twilley et al., 2016).

In this study, model parameters such as the critical bed shear stress for erosion and erosion rate were calibrated and validated using measurements of waves, water levels, SSC, and sediment depositions in 2015 and 2016. Hydrodynamic and sediment transport data were recorded by a tripod deployed at the T1 station located in the middle of FLB during the summer and winter of 2015 and spring of 2016 (Wang et al., 2018). The measurements included significant wave height (H_s), current velocity, water level, and SSC. Wave data were analyzed using the toobox from Karimpour and Chen (2017). Before executing the spectral analysis, Wang et al. (2018) corrected pressure attenuation in the water column based on depth. They also removed spikes in the ADV current data before the velocity analysis, following Goring and Nikora (2002) and Wahl (2003). The WAFO (Wave Analysis for Fatigue and Oceanography) toolbox was employed to determine the periodicities of benthic suspended sediment concentration, as described by Brodtkorb et al. (2000). Furthermore, push cores were collected at ten locations within the study site every two months between May 2015 and May 2016 (Restreppo et al., 2019), as shown in Fig. 1 (c). Five push cores were taken along the center of the bay (FLB1-5), while the other five were collected from adjacent seasonally inundated marsh sites on the eastern edge of the bay (FLM1-5). To determine the ⁷Be inventories, Restreppo et al. (2019) measured the grain density of dry, powdered samples using a Quantachrome Ultrapyc 1200e gas pycnometer. Then they computed inventories of ⁷Be to assess the morphological change rate at different sites within the bay. The simulated and measured data of H_s, current velocity, water level, SSC, and deposition rate were compared to evaluate the accuracy of the model. Error statistics such as root-mean-square error (RMSE) and correlation of determination (R^2) were used to quantify the correlation between the simulated and measured data. For detailed information about the processing of the field data, the reader is referred to Wang et al. (2018) and Restreppo et al. (2019).

2.2. Model settings

2.2.1. Model description

The Delft3D modeling suite was employed to simulate hydrodynamics and sediment transport for exploring the sediment flux and morphological changes in FLB and the surrounding wetlands. Delft3D is a multi-dimensional modeling suite used for estimating waves, flows, sediment transport, morphological change, water quality, and ecology in various aquatic environments, including shallow seas, coastal areas, lakes, rivers, and estuaries (e.g., Lesser et al., 2004; Hu et al., 2009; Benedet et al., 2016). The primary component of the Delft3D modeling suite is Delft3D-FLOW, which solves the Navier-Stokes equation for incompressible non-steady flow under shallow water and Boussinesq assumptions (Deltares, 2023). The model incorporates the influence of waves on flow and sediment transport through online coupling with Delft3D-WAVE (i.e., SWAN, Booij et al., 1999). SWAN is a state-of-the-art third-generation spectral wave model that has been developed to accurately forecast the generation and transformation of wind waves in coastal waters (Holthuijsen et al., 2004). By solving the wave action balance equation, SWAN is capable of calculating the temporal, geographical, and spectral evolution of wave spectra. In the modeling system, Delft3D-FLOW plays a crucial role by providing SWAN with essential inputs, including water level and current velocity data. Based on these inputs, SWAN generates wave parameters that are used to compute radiation stresses and wave-current bed shear stress. These calculations, in turn, impact the water levels and velocities within the Delft3D-FLOW model. To account for sediment transport and

morphology, Delft3D-FLOW incorporates the sediment transport and morphology modules, which enable the calculation of both bedload and suspended load transport for non-cohesive sediment (sand), as well as suspended load transport for cohesive sediment (mud). In this study, the model focuses exclusively on fine sediment (mud). The sediment fluxes between the water phase and the bed were computed using the Partheniades-Krone method (Partheniades, 1965). This method provides a reliable framework for estimating the movement of sediment particles within the model, allowing for a comprehensive analysis of sediment dynamics.

2.2.2. Model domains

In this study, a two-dimensional Delft3D model was employed to investigate the depth-integrated sediment fluxes and morphological changes in FLB. This is because FLB is a shallow and vertically wellmixed estuary, and the two-dimensional model has better computational efficiency. Nested three-level computational domains were developed for the simulations. The first level GoM domain encompassed the GoM itself and a portion of the North Atlantic Ocean and the Caribbean Sea (Fig. 1 (a)). To define the boundary conditions for this domain, the model incorporated seven primary tidal constituents, including O1, K1, Q1, M2, N2, S2, and K2. The second level domain spanned from the west of Vermillion Bay to the east of Caillou Bay (Fig. 1 (b)). Boundary conditions for water level were obtained from the GoM domain simulation in the south and from two United States Geological Survey (USGS) stations in the north (i.e., Wax Lake Outlet at Calumet (USGS 07381590) and Lower Atchafalaya River at Morgan City (USGS 07381600)).

The third level local domain comprised FLB and the surrounding wetlands (Fig. 1(c)). Water level and current data at the northern, southern, and eastern boundaries were interpolated from the regional domain simulation using the nesting tool offered by the Delft3D model. Sediment transport at the south and north boundaries was driven by imposed time series of sediment concentrations. Since measurement data for sediment concentration at the north boundary were lacking, estimates were derived based on turbidity data from the USGS station at Lower Atchafalaya River in Morgan City (USGS 07381600), which is located 35 km north of the model's northern boundary. The sediment concentration at the north boundary was estimated using the following equation:

$$SSC_{north}(t) = Turb_{USGS}(t - 2 days)/150$$
(1)

The units for the SSC at the north boundary and turbidity at the USGS station are kg/m³ and FNU, respectively. The two-day phase difference was determined by calculating the cross-correlation between the measured turbidity at the USGS station and the observed SSC at the T1 station, assuming that the SSC at the north boundary and T1 station are in phase. Additionally, a calibration factor of 1/150 was applied based on measured SSC at the T1 station and turbidity at the USGS station under fair weather conditions. Overall, the idea was to convert turbidity from the upper river into SSC measured inside the bay, considering that sediment settles out with distance when transported away from the river mouth. At the south boundary, the SSC value was reduced by 50% due to data limitations (i.e., $SSC_{south} = 0.5 \times SSC_{north}$), which was also calibrated based on the measured SSC at the T1 station. The sensitivity of model results to the south boundary conditions was evaluated in Section 4.4. Neumann-type boundary conditions were imposed for sediment at the east boundary.

Full coupling between Delft3D-FLOW and SWAN was implemented only within the local domain simulation as a compromise on computation efficiency. The wind waves were simulated by SWAN every 3 h, and the communication with Delft3D-FLOW happened at the same interval. Since FLB is sheltered from ocean waves (i.e., waves from the GoM) due to its orientation, it was assumed that waves inside the bay were mainly locally generated by winds within the local domain. More details of the domain properties can be found in Table 2.

Table 2Characteristics of the FLB wetland morphology modeling system.

Level	Domain	Size	Grid spacing	Flow time steps
1	GoM	218×210	4–60 km	3 min
2	Regional	1.071×631	50 km	0.5 min
3	Local	400×280	30–80 m	0.5 min

The GoM domain simulation utilized 6-hourly space-varying wind and pressure data from the NCEP/NCAR Reanalysis on the T62 Gaussian grid. For the regional and local domain simulations, hourly wind data from the NOAA station at North of Eugene Island (EINL1-8 764 314) were uniformly applied. Bathymetric data for the local domain and part of the regional domain were obtained from the Coastal National Elevation Dataset (CoNED, U.S. Geological Survey, 2015). To obtain the bathymetry of the GoM and a section of the regional domain, interpolation was conducted based on the ADCIRC mesh (SL16) utilized in prior studies (Dietrich et al., 2011). Additionally, the ADCIRC mesh data were employed to assign Manning's coefficient for all Delft3D domain simulations.

2.2.3. Vegetation effects

In this study, vegetation models were incorporated into Delft3D to consider the influence of different marshes on wave fields and water levels in FLB. Generally, wetland vegetation can be represented using two methods in Delft3D. The first method is commonly used in large-scale simulations. It involves spatially assigning an enhanced Manning's roughness coefficient based on vegetation and land types, which enables a rough classification of different land covers. The second method is based on the trachytope approach, which enables the specification of bed roughness and flow resistance at a sub-grid level by using different roughness classes (Deltares, 2023). In our model, the first method was employed in the GoM domain simulation, while the second method was utilized in the regional and local domains to accurately represent the effects of vegetation on wave attenuation and storm surges.

To implement the trachytope approach, we identified the distribution of vegetation categories based on an aerial survey conducted by USGS in coastal Louisiana in 2013 (Sasser et al., 2014). As a result, four vegetation types were considered in the model, including saline, fresh, brackish, and intermediate marshes (Table 3). The corresponding physical properties were determined based on the USDA NRCS herbaceous plant online database and Liu et al. (2018). As only one type of vegetation is allowed in SWAN (or DWAVE) when online coupling with Delft3D-FLOW, a set of representative vegetation parameters was selected for the study area in the wave model (Hu et al., 2018). The

Table 3
Vegetation properties used in the FLB vegetation model. The vegetation types and common species were obtained from Sasser et al. (2014). The physical properties of various vegetation were estimated based on Liu et al. (2018). Cd and Cb are the bed roughness and drag coefficient, respectively.

Туре	Common Species	Height (m)	Density × diameter (m ⁻¹)	C_d	C _b (m ^{1/} ² /s)
Saline marsh	Spartina alterniflora, Distichlis spicata	0.4	1.25	1.65	33
Fresh marsh	Panicum hemitomon, Sagittaria lancifolia, Eleocharis baldwinii, Cladiumjamaicense.	0.76	3.23	1.65	33
Brackish marsh	Spartina patens	0.5	1.11	1.65	33
Intermediate marsh	Leptochloa fusca, Panicum virgatum, Paspalum vaginatum, Phragmites australis	0.5	4.25	1.65	33

formula proposed by Mendez and Losada (2004) was used in the wave model to account for the influence of vegetation.

2.2.4. Sediment parameters

In this study, only cohesive sediment (mud) was considered in the model (Table 4). In the third level local domain, the calibration of mud parameters was carried out, with the majority of parameters being assigned the default values provided by Delft3D. The critical bed shear stress for sedimentation was assigned a high value of 1 000 N/m², assuming continuous mud deposition (Winterwerp and Van Kesteren, 2004; Hu et al., 2018). Spatially varying values for the critical bed shear stress of erosion were applied based on different vegetation types. Specifically, the values were set at 0.25, 0.3, 0.25, 0.25, 0.11, and 0.4 N/m² for the saline marsh, fresh marsh, brackish marsh, intermediate marsh, water, and swamp, respectively. The values were calibrated based on long-term morphological change data from ten stations (Fig. 6). Specifically, different critical bed shear stresses were applied to various testing cases. Afterward, the sediment deposition output from different models was compared to the measurements at stations FLB 1-5 and FLM 1-5 from May 2015 to May 2016. The optimal model was considered the one that could best simulate the sediment deposition at the study site. As for the settling velocity and erosion rate, constant values were utilized, which were similarly calibrated based on the observed morphological change rate within the FLB.

To evaluate the contribution of various sediment sources in sediment transport within FLB, the local domain simulation considered eight groups of cohesive sediments to distinguish sediment sources (Fig. 1 (d)). These groups were categorized as follows: (I) east wetlands (land areas), (II) west wetlands (land areas), (III) upper bay, (IV) lower bay, (V) north input, (VI) south input, (VII) east wetlands (water areas), and (VIII) west wetlands (water areas). The initial condition for water level was set to zero in the GoM, regional, and local domains. For sediment concentration, the initial value for group (V) north input was set to 0.2 kg/m³, which approximates the sediment concentration in the river, while the other sediment groups were assigned a value of zero. The initial sediment thickness at the bed was set to 1 m, which exceeded the total bed elevation change during the entire model run.

2.3. Sediment flux analysis

To better examine the relationship between sediment fluxes and different driving forces, several study intervals were determined based on river discharge and winds, both of which are closely correlated with sediment transport in FLB and nearby wetlands (e.g., Restreppo et al., 2019). Fig. 2 shows the river discharges at the Atchafalaya River and meteorological data at the study site from May 2015 to May 2016. Typically, river discharge in the fall and winter seasons is lower, while it

Parameters employed for modeling sediment transport within FLB using the Delft3D model.

Cohesive sediment (mud)	
Reference density for hindered settling	1 600 kg/m³ (default)
Specific density	2 650 kg/m ³ (default)
Dry bed density	500 kg/m ³ (default)
Settling velocity	1×10^{-4} m/s (sediment I, II, III, IV, VII, VIII) 1×10^{-5} m/s (sediment V, VI)
Initial thickness at bed	1 m (thick enough)
Critical bed shear stress for sedimentation	1 000 N/m ² (default)
Critical bed shear stress for erosion	Spatially varying (calibrated, based on vegetation type) 0.5 N/m ² (sediment V, VI)
Erosion rate	$2.5\times 10^{-6}~kg/m^2/s$ (sediment I, II) $6.4\times 10^{-6}~kg/m^2/s$ (sediment III, IV, V, VI, VII, VIII)

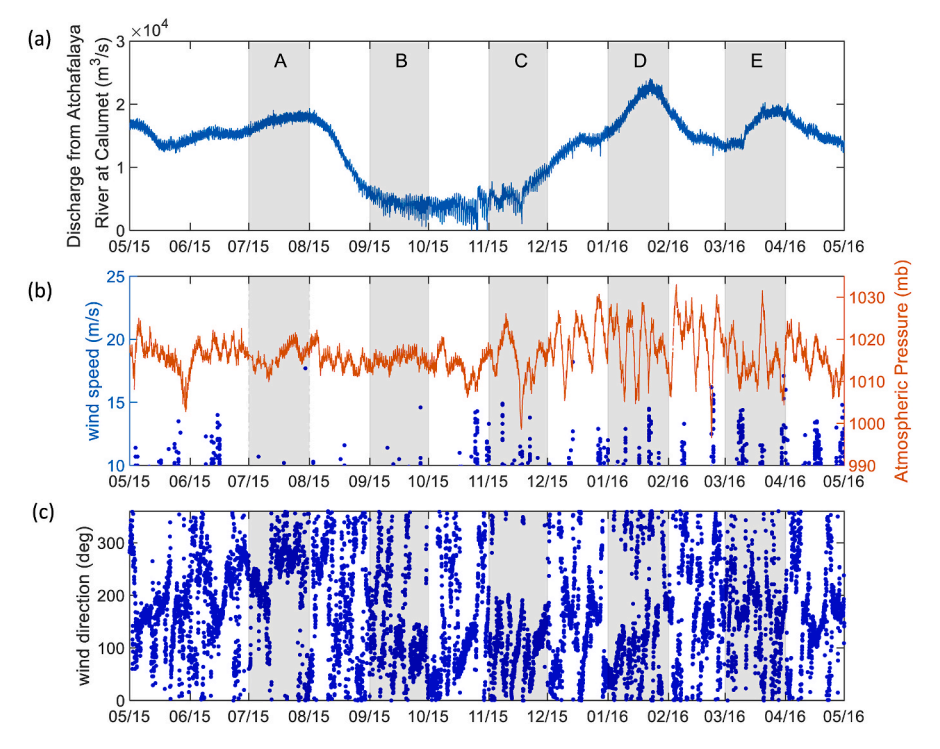


Fig. 2. The river discharges and meteorological conditions at the study site: (a) Discharge data from the USGS station at Wax Lake Outlet at Calumet (USGS 07381590). (b) Wind speed and pressure obtained from the NOAA station at Atchafalaya River at North of Eugene Island (8764314) between May 2015 and May 2016. The columns of blue dots represent wind speeds greater than 10 m/s each day, indicating the passage of storms, especially when a decrease in atmospheric pressure happens simultaneously. (c) Wind direction obtained from the NOAA station at Atchafalaya River at North of Eugene Island (8764314) between May 2015 and May 2016.

is higher in the spring and summer, primarily driven by snow melting upstream and increased precipitation in the MRD (Wang et al., 2018). However, several major floods occurred at our study site, with an abnormally high discharge period between December 2015 and February 2016 (Fig. 2 (a)). Regarding meteorological conditions, more storms occurred after November 2015, characterized by larger atmospheric pressure drops and higher wind speeds (Fig. 2 (b)). In this work, the effect of wind directions (Fig. 2 (c)) on sediment flux was also

considered during the storm season, as strong northerly/southerly winds can increase/reduce the flow into the GoM, considering the geometry of the study site (a northerly wind comes from the north and blows towards the south). Fig. 3 presents wind roses of wind data (the NOAA station at Atchafalaya River at North of Eugene Island (8,764,314)) during each study interval. It can be observed that strong northerly and southerly winds occurred in January and March 2016, respectively. Therefore, a total of five study intervals were determined to investigate the influence

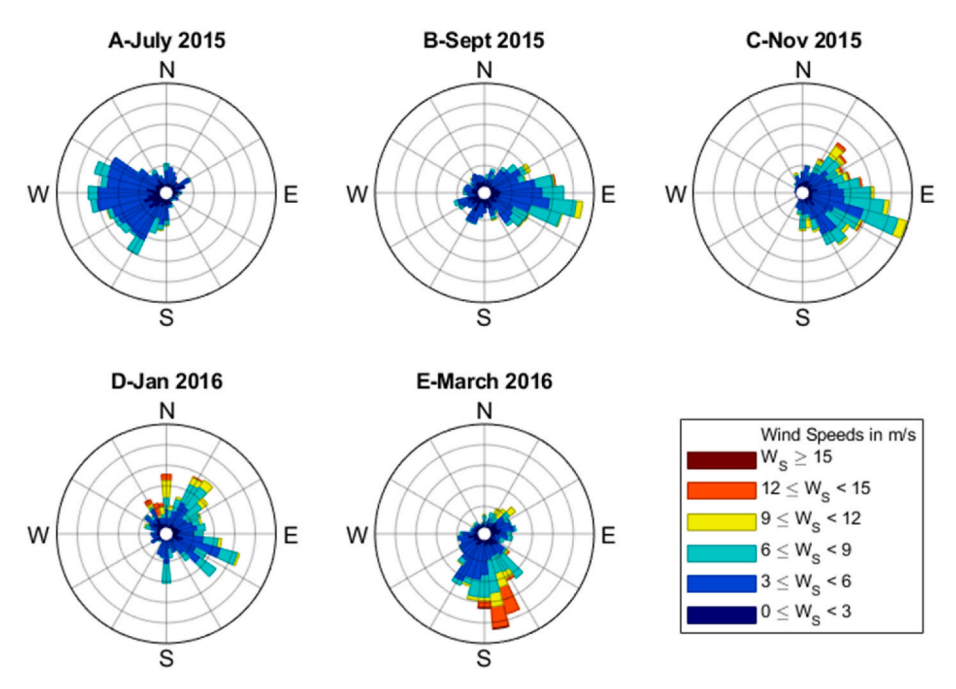


Fig. 3. Wind roses from the NOAA station at Atchafalaya River at North of Eugene Island (8764314) during the five study intervals.

Table 5Five study intervals and the corresponding river discharge and meteorological conditions at the study site in 2015 and 2016.

	Study interval	River discharge and meteorological conditions	
Α	July 2015	high river discharge, a few storms	
B	September 2015	low river discharge, a few storms	
C	November 2015	low river discharge, more storms ^a , weak southerly wind	
D	January 2016	high river discharge, more storms, strong northerly windb	
\boldsymbol{E}	March 2016	high river discharge, more storms, strong southerly wind	

^a 'More storms' means more than three storms per month.

of river discharge and storms on sediment transport (Table 5).

3. Results

3.1. Model validation

As mentioned above, model parameters applied in this study were calibrated and validated using measurements of waves, water levels, SSC, and sediment depositions in 2015 and 2016. Fig. 4 presents a comparison between the observed and modeled water levels at four NOAA stations (station ID: 8764044, 8766072, 8764227, and 8764314, Fig. 1 (b)). The modeled water levels were obtained based on simulations from the regional domain. The R^2 and RMSE values for the simulations at all tide stations are 0.84 and 0.14 m, respectively, indicating that the model can reproduce the water levels.

Fig. 5 shows the comparisons of the observed and simulated water level, current velocity, H_s , and SSC at the T1 station. The simulations were obtained from the local domain. The results show that the modeled H_s are in good agreement with the observations, and the simulated SSC generally follows the measurement trends at the T1 station, suggesting that the wave and morphology models can reasonably estimate the wave

characteristics and sediment transport in FLB.

Furthermore, the model was validated with measurements (Restreppo et al., 2019) of morphological changes at ten stations (i.e., FLB1-5 and FLM1-5) between May 2015 and May 2016 (Fig. 6). The simulated morphological change rates closely match the measured rates at FLM1, FLM2, FLB1, FLB3, FLB4, and FLB5. The modeled rates at FLM3, FLM4, FLM5, and FLB2 also fall within the range of observations. Overall, the simulated morphological changes at the ten stations exhibit a reasonable correlation with the observed ones, indicating that the modeling system can effectively capture the morphological dynamics at the study site.

3.2. Spatial patterns of erosion and deposition in FLB

The annually averaged morphological change rate was simulated to determine the spatial patterns of sediment erosion and deposition in FLB from May 2015 to May 2016 (Fig. 7). The results reveal that morphological change exhibits a spatially varying characteristic. It was found that most erosion occurred in the south and east bayous, as well as in regions close to the eastern and western edges of the bay near the shorelines (Fig. 7 (a)). To better understand the reason for the large erosion along the eastern and western edges of the bay, we compared the initial and final bottom depths at the beginning and end of the simulation along two cross-sections (Fig. 7 (b)). It can be observed that the initial bathymetry of the bay floor was not "smooth" along the transect A-A. Thus, the large erosion near the shorelines and the patchy depositions in the middle of the bay are likely caused by the local variations of the initial bathymetry. Furthermore, we found that erosion is less obvious to the east of transect B-B than to the west. This can be explained by the fact that the bay floor at the beginning of the simulation was smoother to the east than to the west. The sediment deposition also exhibited a spatially varying pattern, mostly occurring in areas adjacent to the eroded regions. A sensitivity test using a smoothed bathymetry

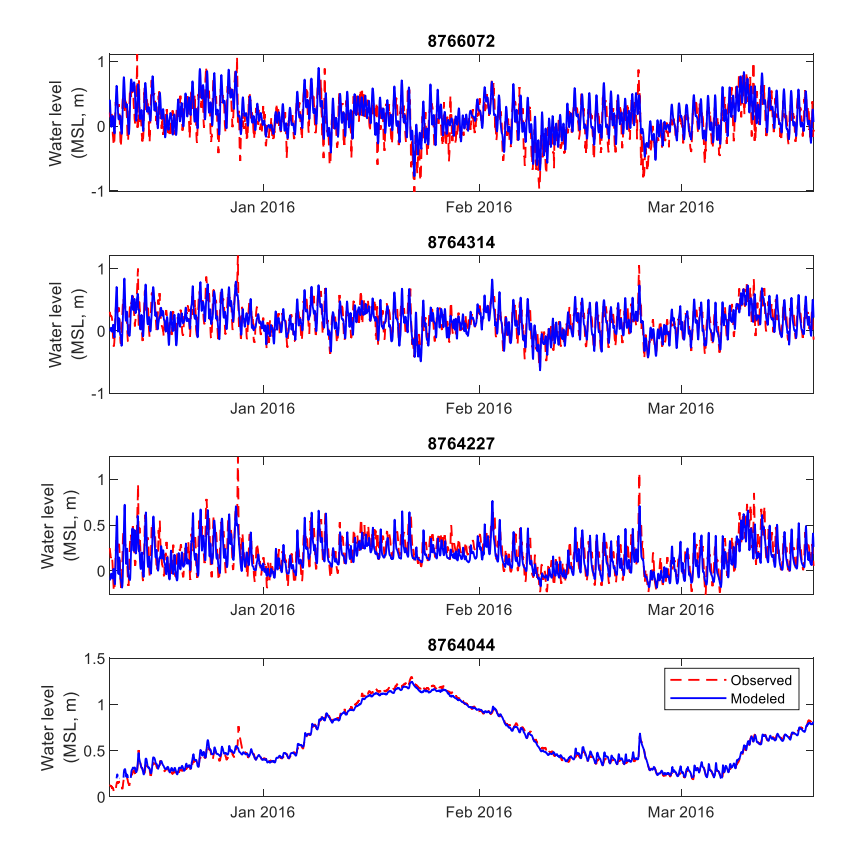


Fig. 4. Comparison between the modeled and measured water levels at the four NOAA stations.

^b 'Strong winds' means wind speed greater than 10 m/s.

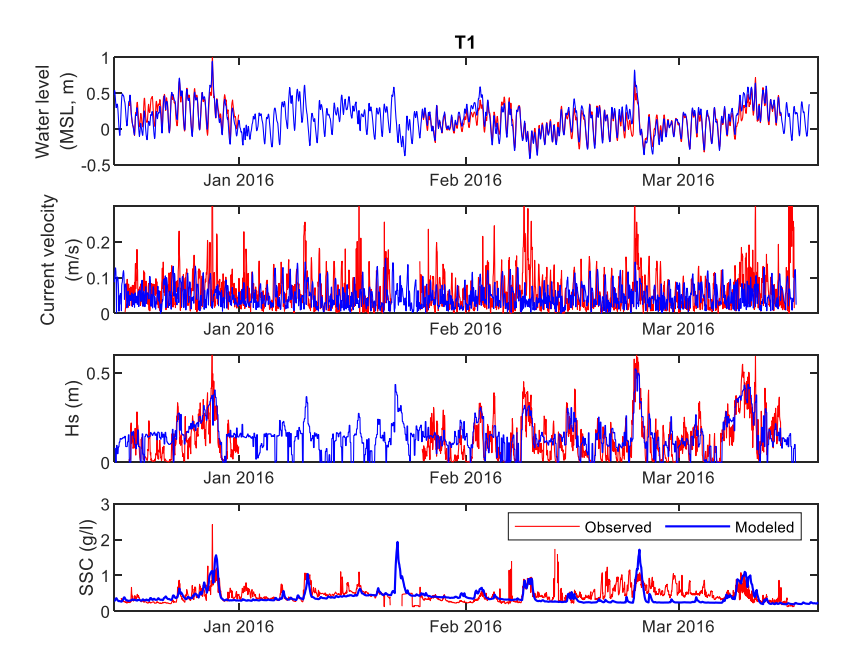


Fig. 5. Comparison between modeled water level, waves, current, and SSC with the observations at the T1 station.

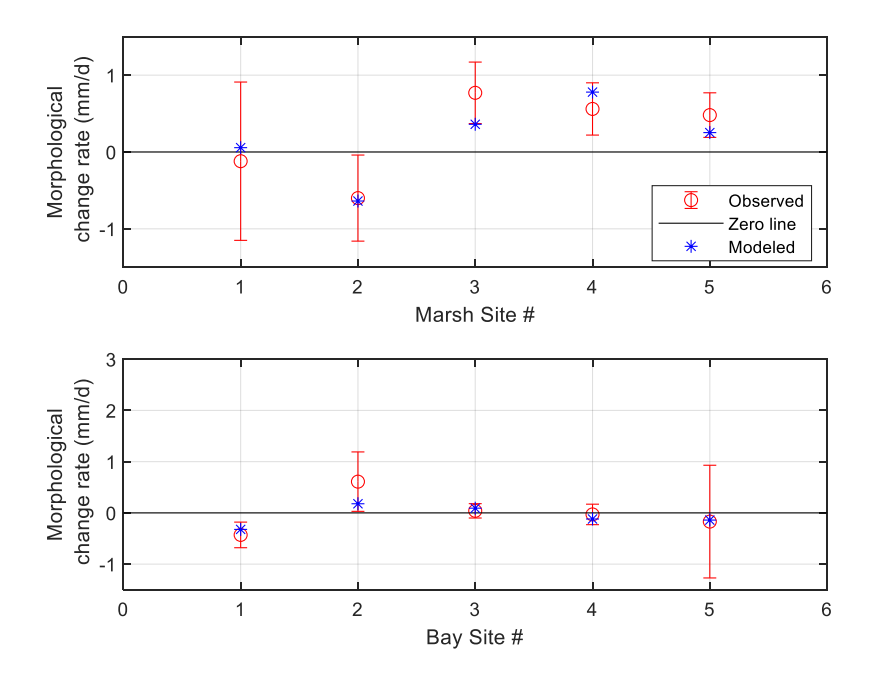


Fig. 6. Comparison between simulated and measured morphological change rates in the marsh and bay areas.

produced the same trend and pattern of sediment fluxes across the bay and wetland boundaries.

4. Discussion

4.1. Sediment fluxes in FLB

To evaluate sediment fluxes within FLB and between the bay and surrounding wetlands, five cross-sections were defined in the local domain simulation (Fig. 8 (f)). Cross-sections Nb and Sb represent the upper and lower boundaries of FLB, which are also the north and south boundaries of the local domain simulation, respectively. Cross-sections

Eb and Wb are located between the bay and the eastern and western wetlands, respectively. Cross-section Cb is positioned between the upper and lower portions of the bay. The cumulative net sediment flux was calculated by integrating the sediment fluxes through the cross-sections Nb, Eb, Sb, and Wb over time.

Fig. 8 shows the cumulative sediment fluxes in the local domain during the five study intervals A-E. Positive values indicate sediment import to the bay, while negative values represent sediment export from the bay. The results indicate that more sediment could be deposited to the eastern and western marshes with high river discharges and strong winds (i.e., January and March 2016). Thus, by strategically aligning the timing of pulses of river water from the diversion with the seasonal

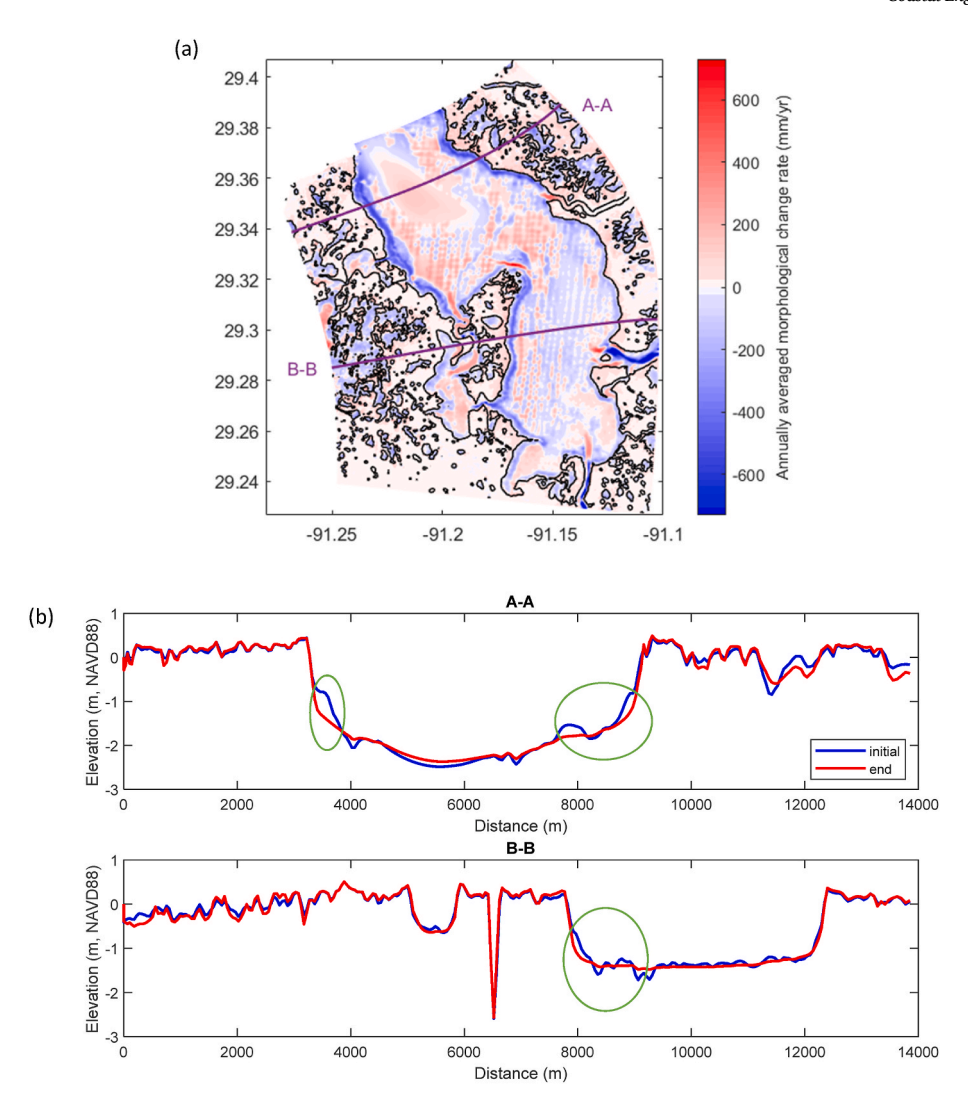


Fig. 7. (a) Simulated annually averaged morphological change rate in FLB from May 2015 to May 2016. The black lines show the locations of the mean sea level shoreline. (b) Bed elevations of two cross-bay transects at the beginning and end of the simulation. The x-axis shows the distance from the origin at the left boundary of the simulation domain. The green circles indicate locations experiencing significant erosion from May 2015 to May 2016.

intensification of atmospheric forcing, it is possible to sustain and promote the growth of the surrounding marshland. We also evaluated the cumulative net sediment fluxes through the four boundaries of the bay during the entire study period (Fig. 8 (f), i.e., May 2015–May 2016). It turns out that sediment removal exceeded sediment deposition on the bay floor, leading to approximately 1 056 KMT (KMT: 1 000 metric tons) of sediment (equivalent to 398,489 $\rm m^3$ in volume, assuming a density of 2 650 kg/m³) being eroded from the bay bottom. As a result, about 1.4 cm of erosion occurred during the entire study period (considering the bay area to be around 95 km² and a porosity of approximately 0.7).

Interestingly, net erosion occurred inside the bay despite the concurrent occurrence of major floods during the study period. According to Perez et al. (2000), The consistent supply of sediment from the Atchafalaya River, along with the substantial resuspension of sediments due to intense winds, played crucial roles in the significant sediment exports observed from FLB. To further examine this feature, we simulated sediment fluxes of each sediment group through different cross-sections in FLB between May 2015 and May 2016 (Fig. 9), as well as during the five study periods (Figure A 1 - Figure A 5). The results indicate that sediment groups III and IV (i.e., resuspended sediment from the upper and lower bay floor) contributed the most to the sediment exported from the bay during the entire study period (Fig. 9). Additionally, it can be observed that the net sediment deposition from the upper river (i.e.,

sediment group V) to the bay system mostly occurred during study periods A, D, and E (i.e., July 2015, January and March 2016), when the river discharge was high (Figure A 1, Figure A 4, and Figure A 5). Overall, the simulation results from our model are consistent with the findings of Perez et al. (2000).

4.2. Sediment fluxes in marshes

Based on the numerical experiments, multiple processes occurred during the study period from May 2015 to May 2016, including the deposition of riverine sediment into the bay, direct deposition of riverine sediment in the marshes, sediment resuspension from the bay floor, and redistribution of suspended sediment to marshes and the GoM. These processes were also observed in the studies of sediment transport by Liu et al. (2018) and Freeman et al. (2015). Fig. 9 shows that sediment deposition in the eastern and western marshes between May 2015 and May 2016 was mainly caused by sediment resuspension from the upper and lower bay floor (i.e., sediment groups III and IV), as well as sediment supply from the upper river (i.e., sediment group V).

To further analyze the sediment fluxes to the surrounding marshes, we generated Table 6 to present the cumulative sediment fluxes to the eastern and western marshes from the eight sediment groups during each study period. The results show that most of the sediment deposition

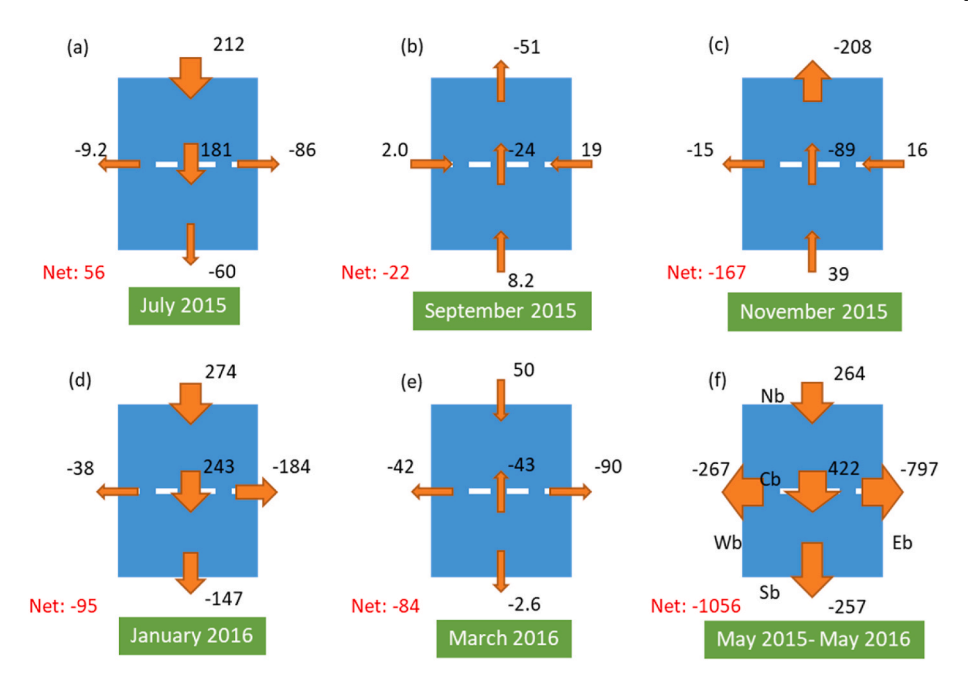


Fig. 8. Simulated cumulative sediment fluxes through different cross-sections in FLB and nearby wetlands with the unit KMT (1 000 metric tons). (a)–(e) Sediment exchanges within the system during different months. (f) Sediment fluxes between May 2015 and May 2016 with the names of the five cross-sections. The blue box represents the bay. Cross-sections Nb and Sb represent the upper and lower boundaries of FLB, which are also the north and south boundaries of the local domain simulation, respectively. Cross-sections Eb and Wb are located between the bay and the eastern and western wetlands, respectively. Cross-section Cb is positioned between the upper and lower portions of the bay.

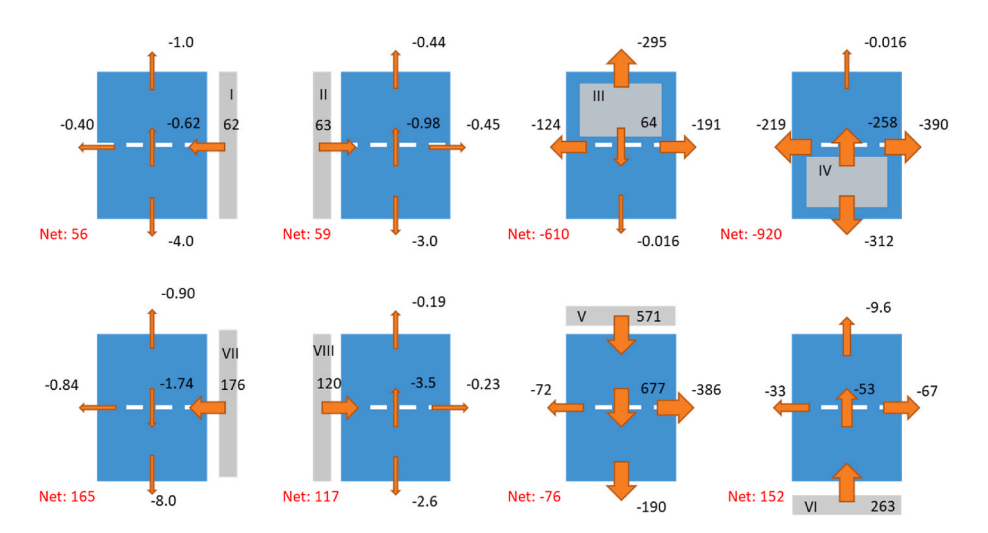


Fig. 9. Simulated cumulative sediment fluxes of each sediment group through different cross-sections in FLB and nearby wetlands between May 2015 and May 2016 with the unit KMT (1 000 metric tons). The gray areas represent the location of the sediment sources (Fig. 1 (d)). The blue box represents the bay.

in the eastern and western marshes occurred during study interval D (January 2016), characterized by strong northerly winds and high river discharge. During this period, significant amounts of resuspended sediments (i.e., sediment groups III and IV) caused by cold front passages were transported from the bay to the marshes. Meanwhile, a substantial amount of riverine sediments (i.e., sediment group V) were directly deposited into the marshes. Furthermore, we found that riverine sediments were more likely to be directly deposited into the marshes when the river discharge was high (i.e., July 2015, January 2016, and March 2016), accounting for over 40% of the total volume of sediment transported from the river to the bay system (Figure A 1, Figure A 4, and

Figure A 5). However, during other study intervals, the riverine sediment was more likely to be initially deposited into the bay, which could later be resuspended and deposited into the marshes during storms or cold fronts. In other words, during calm weather conditions and normal river discharge, FLB acted as a reservoir, storing sediment from the upper river, and later acted as a source of sediment to the nearby wetlands and the GoM during energetic atmospheric conditions. Also, the use of the bay floor as a reservoir can extend the distance over which wetlands can be nourished by sediment diversions, as the wetland sediment supply becomes a multi-step process. These findings are consistent with the analysis conducted by Restreppo et al. (2019).

Table 6
Simulated cumulative sediment fluxes entering (positive values) and leaving (negative values) the eastern and western marshes from eight sediment groups during different study periods with the unit KMT (1 000 metric tons).

Sediment groups	A: Jul 2015	<i>B</i> : Sept 2015	C: Nov 2015	<i>D</i> : Jan 2016	<i>E</i> : Mar 2016	Mar 2015–Mar 2016
I	-2.42	-1.53	-3.26	-3.76	-7.77	-61.31
II	-0.62	-2.06	-5.04	-6.00	-6.36	-62.23
III	2.74	2.92	16.82	20.81	57.72	315.81
IV	8.83	5.20	22.32	106.60	59.07	608.58
V	93.25	0.38	2.11	114.96	42.59	457.47
VI	1.85	2.93	8.79	5.88	11.84	100.35
VII	-5.30	-21.51	-29.30	-3.82	-14.41	-174.82
VIII	-2.64	-7.71	-13.38	-12.35	-10.42	-120.20
Sum (KMT/ day)	3.19	-0.71	-0.03	7.41	4.41	2.91

The time series of cumulative sediment fluxes through different cross-sections from May 2015 to May 2016 is shown in Fig. 10. The numerical simulation reveals that more sediment can be deposited in the eastern and western wetlands through cross-sections Eb and Wb during energetic atmospheric conditions (i.e., after November 2015). Despite the potential decrease in water level inside FLB caused by northerly winds (Perez et al., 2000; Wang et al., 2018), it appears that the water level remained high enough to facilitate sediment deposition in the marshes, regardless of southerly or northerly winds at the study site after November 2015.

Overall, the sediment resuspension from both the upper and lower sections of the bay floor, coupled with the sediment supply from the upper river to the adjacent marshlands, contributes to the relatively stable shoreline or marsh edges of the bay. Moreover, because of the short fetches, the simulated annual averaged wave power near the marsh edge is very low (e.g., 1.4 and 1.9 W/m at FLM3 and FLM5, respectively). Thus, despite the adversities presented by land subsidence, sea level rise, and strong winds, analyses of vertical accretion

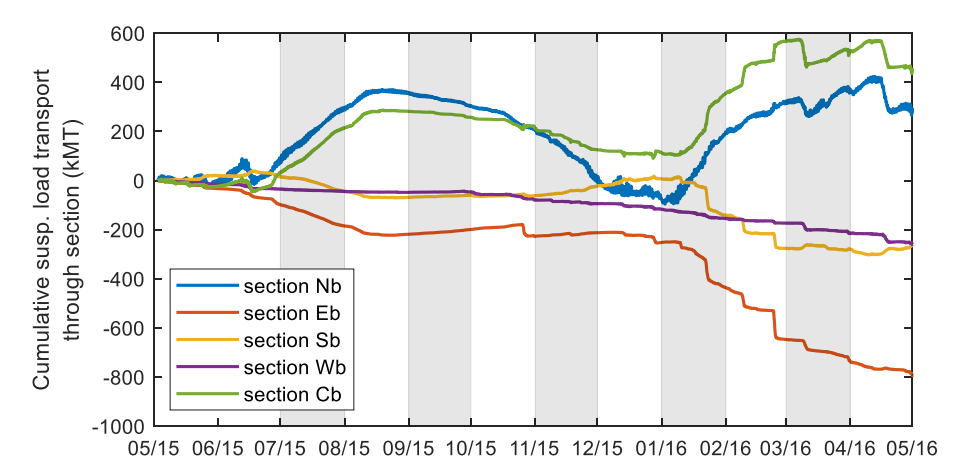


Fig. 10. Simulated cumulative sediment fluxes through each cross-section from May 2015 to May 2016.

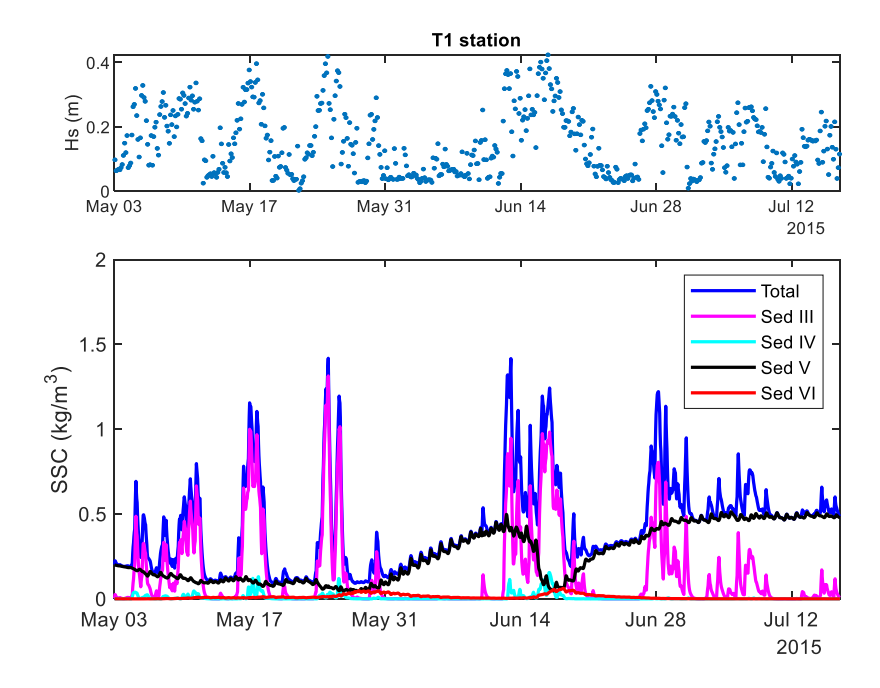


Fig. 11. Simulated wave conditions and contribution of different sediment groups to SSC at T1 station from May to June 2015. The SSC from the sediment groups I, II, VII, and VIII are not shown in the figure because the values are too small to observe.

rates, maps, and satellite imagery indicate no notable shoreline regression or advancement at the study site between the years 1937 and 2010 (Twilley et al., 2016; Wang et al., 2018; Restreppo et al., 2019).

4.3. Contributions of different sediment sources to SSC

Fig. 11 presents the simulated contribution of different sediment groups to SSC at the T1 station from May to June 2015. The SSC at the T1 station varied between 0.09 and 1.46 kg/m 3 . The highest SSC values were observed during severe weather conditions characterized by large waves within the bay, whereas the lowest values occurred during calm periods. Furthermore, it can be observed that the external input (from Atchafalaya Bay/River, i.e., sediment group V) dominated the sediment transport at the T1 station in fair weather conditions with small waves. Conversely, local resuspended sediments (sediment group III) contributed the most to SSC at the T1 station during severe weather with large waves within the bay.

4.4. Influence of south boundary condition of SSC on the model results

In this section, we investigated the sensitivity of the model results to the south boundary conditions of SSC. Multiple simulation experiments were conducted with different ratios between SSC_{south} and SSC_{north}, including $SSC_{south}/SSC_{north} = 0.25, 0.5, 0.75, 1$, and 1.5. It is evident that a ratio smaller than one is more realistic, as there have been no sediment supplies from the river connecting to Terrebonne Bay and Barataria Bay since the 1920s. Supporting our assumption, photos from the Google Earth Engine also depict higher turbidity near the north boundary than the Gulf water near the south boundary. Fig. 12 shows the cumulative sediment fluxes between May 2015 and May 2016 simulated with different sediment boundary conditions at the south. It can be observed that the sediment fluxes through the various sections are not overly sensitive to the sediment boundary conditions at the south, except for Sb. Additionally, we compared the volume of sediment transported through Eb and Wb originating from the river. The results indicate that the sediment boundary conditions at the south do not significantly influence the sediment fluxes from the river (i.e., sediment group V) towards the east (ranging from 365.6 to 388.7 kMT) and west (ranging from 71.5 to 71.9 kMT) cross-sections from May 2015 to May 2016. These findings suggest that the Delft3D simulation results and our findings are not overly sensitive to the sediment boundary conditions at

the south. Direct measurements of SSC at the north and south boundaries are highly recommended in future studies.

5. Conclusions

Fourleague Bay (FLB) has been recognized as an ideal location for investigating the effects of fine sediment diversion strategies in the Mississippi River Delta (MRD). In this study, we utilized the coupled flow-wave Delft3D model to quantitatively assess the hydrodynamic characteristics, sediment transport, and associated morphological changes in FLB. The objective was to enhance our understanding of the dispersal process of fine sediment in the region. The model results exhibit satisfactory agreement between the simulated and observed data for water levels, integral wave parameters, current velocities, and morphological change rates. This indicates that the model effectively captures the hydrodynamic forcings and qualitatively reproduces the sediment transport processes at the study site.

The simulated morphological change rates show strong spatial variability in FLB in 2015 and 2016. The results show that most of the erosion occurred in the south and east bayous and the regions close to the eastern and western edges of the bay (likely caused by the local variations of the initial bathymetry). Additionally, we found that more sediment could be deposited to the eastern and western marshes with high river discharges and strong winds (i.e., January and March 2016). Thus, by strategically aligning the timing of pulses of river water from the diversion with the seasonal intensification of atmospheric forcing, it is possible to sustain and potentially promote the growth of the surrounding marshland. To further examine the processes of sediment transport at the study site, eight groups of cohesive sediments were considered in the FLB simulation to differentiate sediment sources. The contribution of different sediment groups to the suspended sediment concentration was analyzed at the T1 station from May to June 2015. It was found that the external input (mainly from the Atchafalaya Bay/ River, i.e., sediment group V) dominated sediment transport in fair weather conditions. In contrast, local resuspended sediments contributed the most (i.e., sediment group III) during severe weather with large wind waves inside the bay.

Based on the numerical experiments, it was found that multiple processes happened during the study period, including the riverine sediment deposited into the bay, riverine sediment deposited directly in the marshes, resuspension of sediment from the bay floor, and

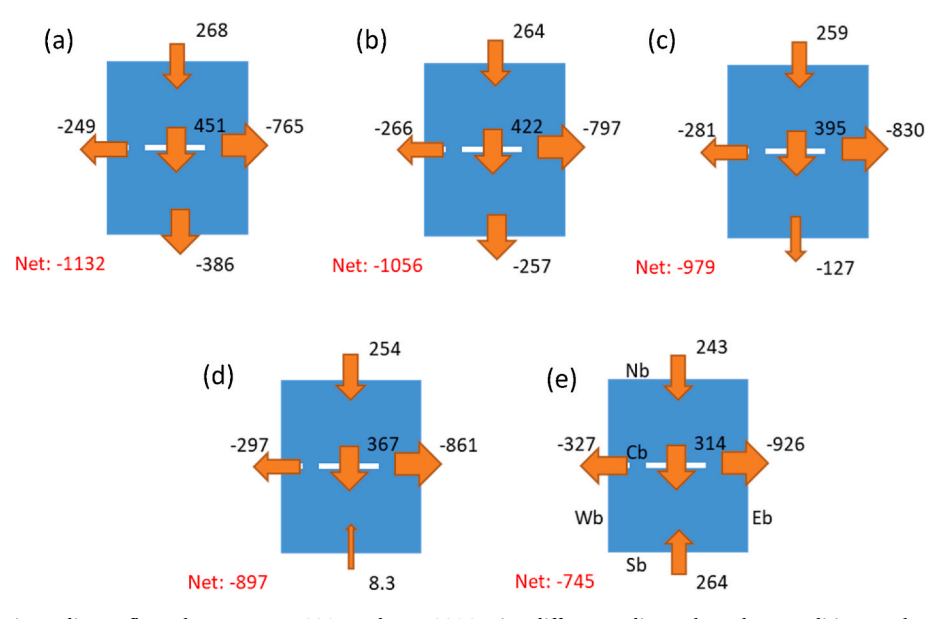


Fig. 12. Simulated cumulative sediment fluxes between May 2015 and May 2016 using different sediment boundary conditions at the south with the unit KMT (1 000 metric tons). (a)–(e) Sediment exchanges within the system with $SSC_{south}/SSC_{north} = 0.25$, 0.5, 0.75, 1, and 1.5, respectively.

redistribution of suspended sediment to marshes and the GoM. The results show that the sediment deposition in the eastern and western marshes of the FLB was mostly caused by the sediment resuspension from the upper and lower bay floor as well as sediment supply from the upper river through the north boundary. The riverine sediment tended to be directly deposited in the marshes when the river discharge was high. However, during other study intervals, the riverine sediment was more likely to be deposited into the bay first, which was later delivered to the marshes during storms or cold fronts. In other words, during calm weather conditions and normal river discharge, FLB behaved as a reservoir to store the sediment from the upper river and later acted as a source of sediment to the nearby wetlands and the GoM during the energetic atmospheric conditions. This suggests that using the bay floor as a reservoir can extend the distance over which wetlands can benefit from the sediment diversions, as the supply of sediment to the wetlands becomes a multi-step process. Therefore, it is important to retain sediments from river divisions in shallow bays, allowing storms to redistribute them to adjacent wetlands.

Overall, the coupled flow-wave Delft3D model guided by in-situ observations shows a good performance for simulating the observed water levels, waves, currents, sediment transport, and morphological changes in FLB. The validated model can be further applied to evaluate the design and operation strategies of sediment diversion projects, such as determining time intervals for opening the diversions and optimal plant characteristics for increasing sediment deposition in the surrounding marshes.

CRediT authorship contribution statement

Nan Wang: Methodology, Software, Data curation, Writing -

original draft. Qin Chen: Conceptualization, Methodology, Validation, Writing, Supervision, Funding acquisition. Kelin Hu: Methodology, Software, Writing – review & editing. Kehui Xu: Investigation, Data curation, Writing – review & editing. Samuel J. Bentley: Investigation, Data curation, Writing – review & editing. Jiaze Wang: Investigation, Data curation, Writing – review & editing.

Declaration of competing interest

The authors declare that they have no known competing financial interests or personal relationships that could have appeared to influence the work reported in this paper.

Data availability

Data will be made available on request.

Acknowledgments

This paper is based upon work supported by the U.S. National Science Foundation under Award No. 1427389/2052443/2139882. Any opinions, findings and conclusions or recommendations expressed in this paper are those of the authors and do not necessarily reflect the views of the National Science Foundation. Any use of trade, firm, or product names is for descriptive purposes only and does not imply endorsement by the U.S. Government. Computational resources were provided by the LSU High Performance Computing (HPC) and Northeastern University HPC facility.



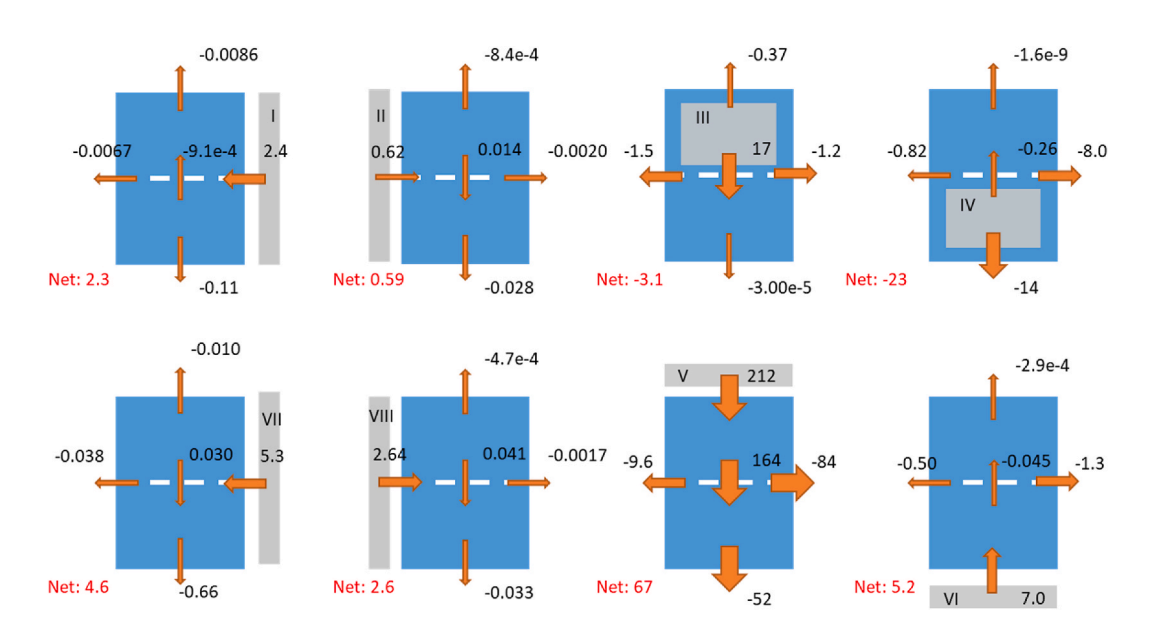


Fig. A1. Cumulative sediment fluxes of each sediment group through different cross-sections in FLB and nearby wetlands during study period A (i.e., July 2015) with the unit KMT (1 000 metric tons). The gray areas represent the location of the sediment sources (Fig. 1 (d)).

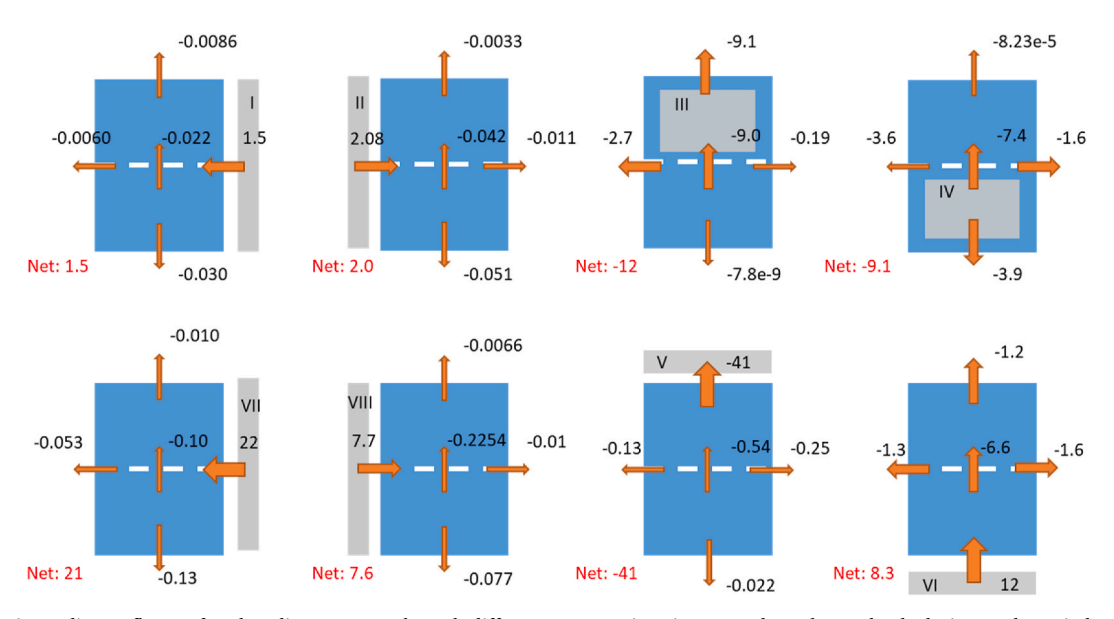


Fig. A2. Cumulative sediment fluxes of each sediment group through different cross-sections in FLB and nearby wetlands during study period B (i.e., September 2015) with the unit KMT (1 000 metric tons). The gray areas represent the location of the sediment sources (Fig. 1 (d)).

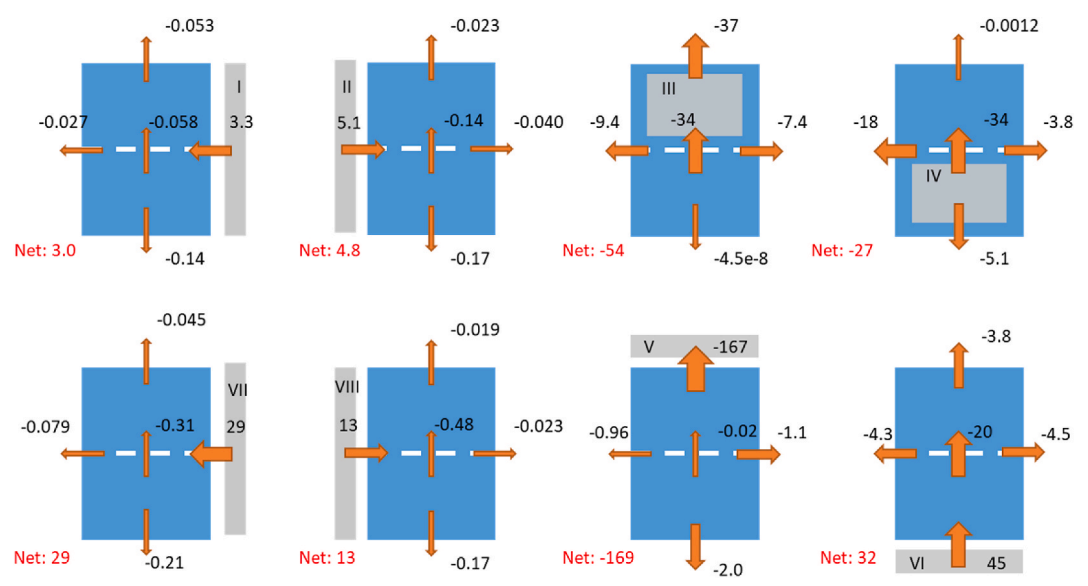


Fig. A3. Cumulative sediment fluxes of each sediment group through different cross-sections in FLB and nearby wetlands during study period C (i.e., November 2015) with the unit KMT (1 000 metric tons). The gray areas represent the location of the sediment sources (Fig. 1 (d)).

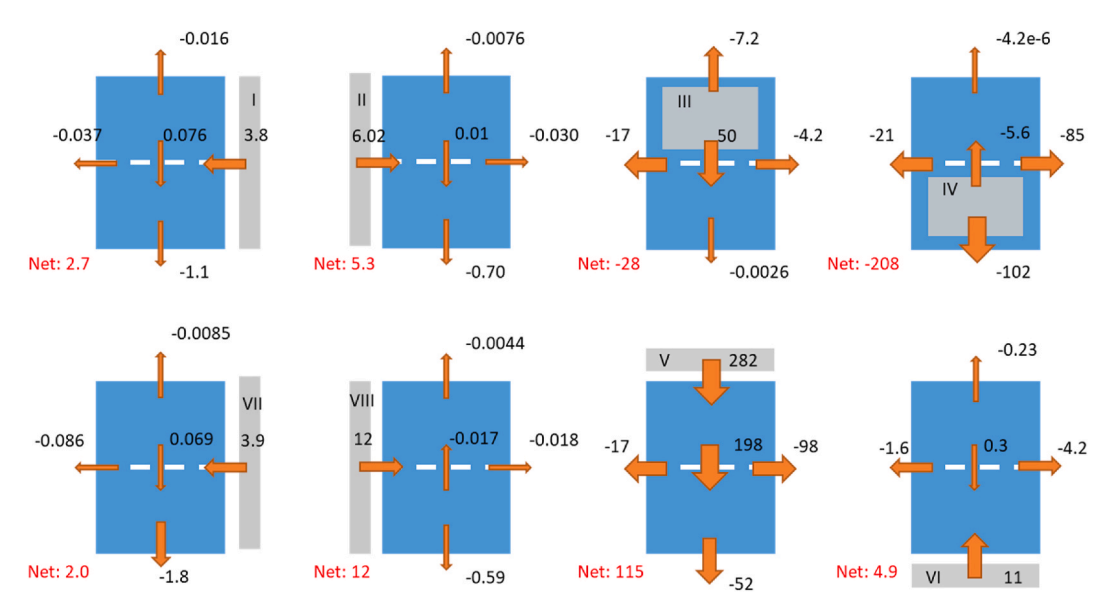


Fig. A4. Cumulative sediment fluxes of each sediment group through different cross-sections in FLB and nearby wetlands during study period D (i.e., January 2016) with the unit KMT (1 000 metric tons). The gray areas represent the location of the sediment sources (Fig. 1 (d)).

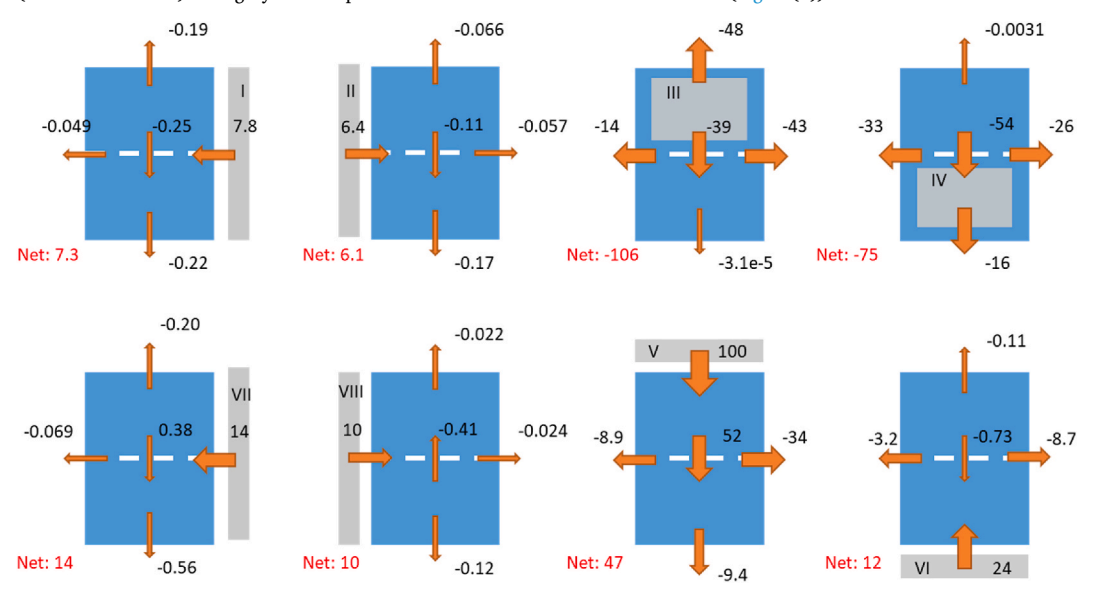


Fig. A5. Cumulative sediment fluxes of each sediment group through different cross-sections in FLB and nearby wetlands during study period E (i.e., March 2016) with the unit KMT (1 000 metric tons). The gray areas represent the location of the sediment sources (Fig. 1 (d)).

References

Benedet, L., Dobrochinski, J.P.F., Walstra, D.J.R., Klein, A.H.F., Ranasinghe, R., 2016. A morphological modeling study to compare different methods of wave climate schematization and evaluate strategies to reduce erosion losses from a beach nourishment project. Coast. Eng. 112, 69–86.

Bergillos, R.J., Masselink, G., Ortega-Sánchez, M., 2017. Coupling cross-shore and longshore sediment transport to model storm response along a mixed sand-gravel coast under varying wave directions. Coast. Eng. 129, 93–104. https://doi.org/ 10.1016/j.coastaleng.2017.09.009.

Bomer, E.J., Bentley, S.J., Hughes, J.E.T., Wilson, C.A., Crawford, F., Xu, K., 2019. Deltaic morphodynamics and stratigraphic evolution of middle Barataria bay and middle Breton sound regions, Louisiana, USA: implications for river-sediment diversions. Estuar. Coast Shelf Sci. 224, 20–33.

Booij, N., Ris, R.C., Holthuijsen, L.H., 1999. A third-generation wave model for coastal regions: 1. Model description and validation. J. Geophys. Res. Ocean. 104, 7649–7666.

Boudet, L., Sabatier, F., Radakovitch, O., 2017. Modelling of sediment transport pattern in the mouth of the Rhone delta: role of storm and flood events. Estuar. Coast Shelf Sci. 198, 568–582. Brodtkorb, P.A., Johannesson, P., Lindgren, G., Rychlik, I., Rydén, J., Sjö, E., 2000. WAFO-a Matlab toolbox for analysis of random waves and loads. In: ISOPE International Ocean and Polar Engineering Conference. ISOPE–I.

Couvillion, B.R., Beck, H., Schoolmaster, D., Fischer, M., 2017. Land Area Change in Coastal Louisiana (1932 to 2016.

CPRA, 2023. Louisiana's Comprehensive Master Plan for a Sustainable Coast. Coastal Protection and Restoration Authority of Louisiana. Baton Rouge, LA.

CPRA, 2017. Louisiana's Comprehensive Master Plan for a Sustainable Coast. Coastal Protection and Restoration Authority of Louisiana. Baton Rouge, LA.

CPRA, 2012. Louisiana's Comprehensive Master Plan for a Sustainable Coast. Coast. Prot. Restor. Auth. Louisiana, Bat. Rouge, Louisiana.

Deltares, D., 2023. Delft3D-FLOW. user manual [WWW Document]. URL. https://content.oss.deltares.nl/delft3d4/Delft3D-FLOW_User_Manual.pdf.

Denes, T.A., Caffrey, J.M., 1988. Changes in seasonal water transport in a Louisiana estuary, Fourleague Bay, Louisiana. Estuaries 11, 184–191.

Dietrich, J.C., Westerink, J.J., Kennedy, A.B., Smith, J.M., Jensen, R.E., Zijlema, M., Holthuijsen, L.H., Dawson, C., Luettich, R.A., Powell, M.D., others, 2011. Hurricane Gustav (2008) waves and storm surge: hindcast, synoptic analysis, and validation in southern Louisiana. Mon. Weather Rev. 139, 2488–2522.

Dissanayake, D.M.P.K., Wurpts, A., Miani, M., Knaack, H., Niemeyer, H.D., Roelvink, J. A., 2012. Modelling morphodynamic response of a tidal basin to an anthropogenic effect: ley Bay, East Frisian Wadden Sea – applying tidal forcing only and different

- sediment fractions. Coast. Eng. 67, 14–28. https://doi.org/10.1016/j.coastaleng.2012.04.001.
- Elsey-Quirk, T., Graham, S.A., Mendelssohn, I.A., Snedden, G., Day, J.W., Twilley, R.R., Shaffer, G., Sharp, L.A., Pahl, J., Lane, R.R., 2019. Mississippi river sediment diversions and coastal wetland sustainability: synthesis of responses to freshwater, sediment, and nutrient inputs. Estuar. Coast Shelf Sci. 221, 170–183.
- Freeman, A.M., Jose, F., Roberts, H.H., Stone, G.W., 2015. Storm induced hydrodynamics and sediment transport in a coastal Louisiana lake. Estuar. Coast Shelf Sci. 161, 65–75.
- Goring, D.G., Nikora, V.I., 2002. Despiking acoustic Doppler velocimeter data. J. Hydraul. Eng. 128, 117–126.
- Herrling, G., Winter, C., 2018. Tidal inlet sediment bypassing at mixed-energy barrier islands. Coast. Eng. 140, 342–354.
- Holthuijsen, L.H., Booij, N., Ris, R.C., Haagsma, I.J.G., Kieftenburg, A., Kriezi, E.E., Ziijlema, M., der Westhuysen, A.J., 2004. SWAN Cycle III Version 40.11 User Manual. Delft Univ. Technol. Press, Delft, Netherlands.
- Hu, K., Chen, Q., Wang, H., Hartig, E.K., Orton, P.M., 2018. Numerical modeling of salt marsh morphological change induced by Hurricane Sandy. Coast. Eng. 132, 63–81.
- Hu, K., Ding, P., Wang, Z., Yang, S., 2009. A 2D/3D hydrodynamic and sediment transport model for the Yangtze Estuary, China. J. Mar. Syst. 77, 114–136.
- Johnson, C.L., Chen, Q., Ozdemir, C.E., Xu, K., McCall, R., Nederhoff, K., 2021. Morphodynamic modeling of a low-lying barrier subject to hurricane forcing: the role of backbarrier wetlands. Coast. Eng. 167, 103886.
- Karimpour, A., Chen, Q., 2017. Wind wave analysis in depth limited water using OCEANLYZ, A MATLAB toolbox. Comput. Geosci. 106 https://doi.org/10.1016/j. cageo.2017.06.010.
- King, E.V., Conley, D.C., Masselink, G., Leonardi, N., McCarroll, R.J., Scott, T., Valiente, N.G., 2021. Wave, tide and topographical controls on headland sand bypassing. J. Geophys. Res. Ocean. 126, e2020JC017053.
- Lane, R.R., Madden, C.J., Day, J.W., Solet, D.J., 2011. Hydrologic and nutrient dynamics of a coastal bay and wetland receiving discharge from the Atchafalaya River. Hydrobiologia 658, 55–66.
- Lesser, G.R., Roelvink, J.A. v, van Kester, J.A.T.M., Stelling, G.S., 2004. Development and validation of a three-dimensional morphological model. Coast. Eng. 51, 883–915.
- Liu, K., Chen, Q., Hu, K., Xu, K., Twilley, R.R., 2018. Modeling hurricane-induced wetland-bay and bay-shelf sediment fluxes. Coast. Eng. 135, 77–90.
- López-Ramade, E., Mulligan, R.P., Medell\`in, G., Torres-Freyermuth, A., 2023.

 Modelling beach morphological responses near coastal structures under oblique waves driven by sea-breezes. Coast. Eng. 182, 104290.
- Luan, H.L., Ding, P.X., Wang, Z.B., Yang, S.L., Lu, J.Y., 2018. Morphodynamic impacts of large-scale engineering projects in the Yangtze River delta. Coast. Eng. 141, 1–11.
- Luijendijk, A.P., Ranasinghe, R., de Schipper, M.A., Huisman, B.A., Swinkels, C.M., Walstra, D.J.R., Stive, M.J.F., 2017. The initial morphological response of the Sand Engine: a process-based modelling study. Coast. Eng. 119, 1–14.
- Mendez, F.J., Losada, I.J., 2004. An empirical model to estimate the propagation of random breaking and nonbreaking waves over vegetation fields. Coast. Eng. 51, 103–118.
- Meselhe, E., Khalifa, A.M., Hu, K., Lewis, J., Tavakoly, A.A., 2021. Influence of key environmental drivers on the performance of sediment diversions. Water 14, 24.
- Meselhe, E.A., Georgiou, I., Allison, M.A., McCorquodale, J.A., 2012. Numerical modeling of hydrodynamics and sediment transport in lower Mississippi at a proposed delta building diversion. J. Hydrol. 472, 340–354.
- Partheniades, E., 1965. Erosion and deposition of cohesive soils. J. Hydraul. Div. 91, 105–139.

- Perez, B.C., Day Jr., J.W., Rouse, L.J., Shaw, R.F., Wang, M., 2000. Influence of Atchafalaya River discharge and winter frontal passage on suspended sediment concentration and flux in Fourleague Bay, Louisiana. Estuar. Coast Shelf Sci. 50, 221, 200
- Restreppo, G.A., Bentley, S.J., Wang, J., Xu, K., 2019. Riverine sediment contribution to distal deltaic wetlands: Fourleague Bay, LA. Estuar. Coast 42, 55–67.
- Rosen, T., Xu, Y.J., 2014. A hydrograph-based sediment availability assessment: implications for Mississippi River sediment diversion. Water 6, 564–583.
- Sasser, C., Visser, J., Mouton, E., Linscombe, J., Hartley, S., 2014. Vegetation Types in Coastal Louisiana in 2013.
- Stevens, A.W., Moritz, H.R., Elias, E.P.L., Gelfenbaum, G.R., Ruggiero, P.R., Pearson, S. G., McMillan, J.M., Kaminsky, G.M., 2023. Monitoring and modeling dispersal of a submerged nearshore berm at the mouth of the Columbia River, USA. Coast. Eng. 181, 104285 https://doi.org/10.1016/j.coastaleng.2023.104285.
- Ton, A.M., Vuik, V., Aarninkhof, S.G.J., 2023. Longshore sediment transport by large-scale lake circulations at low-energy, non-tidal beaches: a field and model study. Coast. Eng. 180, 104268.
- Tonnon, P.K., Huisman, B.J.A., Stam, G.N., van Rijn, L.C., 2018. Numerical modelling of erosion rates, life span and maintenance volumes of mega nourishments. Coast. Eng. 131, 51–69. https://doi.org/10.1016/j.coastaleng.2017.10.001.
- Twilley, R.R., Bentley, S.J., Chen, Q., Edmonds, D.A., Hagen, S.C., Lam, N.S.-N., Willson, C.S., Xu, K., Braud, D., Peele, R.H., others, 2016. Co-evolution of wetland landscapes, flooding, and human settlement in the Mississippi River Delta Plain. Sustain. Sci. 11, 711–731.
- U.S. Geological Survey, 2015. Coastal national elevation database (CoNED) applications project: U.S. Geological survey coastal and marine geology program (CMGP) [WWW Document]. URL. https://topotools.cr.usgs.gov/coned/index.php.
- van Ormondt, M., Nelson, T.R., Hapke, C.J., Roelvink, D., 2020. Morphodynamic modelling of the wilderness breach, Fire Island, New York. Part I: model set-up and validation. Coast. Eng. 157, 103621.
- Wahl, T.L., 2003. Discussion of "despiking acoustic Doppler velocimeter data" by derek G. Goring and vladimir I. Nikora. J. Hydraul. Eng. 129, 484–487.
- Wang, F.C., Ransibrahmanakul, V., Tuen, K.L., Wang, M.L., Zhang, F., 1995.
 Hydrodynamics of a tidal inlet in Fourleague bay/atchafalaya bay, Louisiana.
 J. Coast Res. 733–743.
- Wang, J., Xu, K., Restreppo, G.A., Bentley, S.J., Meng, X., Zhang, X., 2018. The coupling of bay hydrodynamics to sediment transport and its implication in micro-tidal wetland sustainability. Mar. Geol. 405, 68–76.
- Wenneker, I., van Dongeren, A., Lescinski, J., Roelvink, D., Borsboom, M., 2011.
 A Boussinesq-type wave driver for a morphodynamical model to predict short-term morphology. Coast. Eng. 58, 66–84. https://doi.org/10.1016/j.coastaleng.2010.08.007.
- Winterwerp, J.C., Van Kesteren, W.G.M., 2004. Introduction to the Physics of Cohesive Sediment Dynamics in the Marine Environment. Elsevier.
- Xu, K., Bentley, S.J., Day, J.W., Freeman, A.M., 2019. A review of sediment diversion in the Mississippi River Deltaic Plain. Estuar. Coast Shelf Sci. 225, 106241.
- Yao, P., Su, M., Wang, Z., van Rijn, L.C., Zhang, C., Stive, M.J.F., 2018. Modelling tidal-induced sediment transport in a sand-silt mixed environment from days to years: application to the Jiangsu coastal water. China. Coast. Eng. 141, 86–106.
- Yuill, B.T., Khadka, A.K., Pereira, J., Allison, M.A., Meselhe, E.A., 2016.
 Morphodynamics of the erosional phase of crevasse-splay evolution and implications for river sediment diversion function. Geomorphology 259, 12–29.
- Zhu, Q., Wiberg, P.L., Reidenbach, M.A., 2021. Quantifying seasonal seagrass effects on flow and sediment dynamics in a back-barrier bay. J. Geophys. Res. Ocean. 126, e2020JC016547.